Accepted Manuscript

Combined THz and LIPS analysis of corroded archaeological bronzes

I. Cacciari, J. Agresti, S. Siano

PII: S0026-265X(15)00331-8
DOI: doi: 10.1016/j.microc.2015.11.051
Reference: MICROC 2350

To appear in: *Microchemical Journal*

Received date: 14 August 2015
Revised date: 26 November 2015
Accepted date: 26 November 2015

Combined THz and LIPS analysis of corroded archaeological bronzes

I. Cacciari*, J. Agresti, S. Siano
Istituto di Fisica Applicata "Nello Carrara" – Consiglio Nazionale delle Ricerche
*Via Madonna del Piano 10, 50019, Sesto Fiorentino (FI), Italy, *i.cacciari@ifac.cnr.it*

Abstract

In this work we have studied corroded archaeological artefacts by combining THz and laser induced plasma spectroscopy (LIPS). The main aim of the work was the assessment of the potential of the THz TDS reflectometry for achieving stratigraphic information and the presence of the metal bulk beneath encrustations and alteration layers before measuring LIPS elemental depth profiles. The behaviour of the reflected THz pulses was formerly investigated by preparing a set of suitable mock-ups, then measurements were carried out on a set of authentic archaeological samples exhibiting different stratigraphic situations, and eventually a deeply corroded Egyptian bronze figurine was characterised. The results achieved show the range of stratigraphic information, which can be provided by THz and the advantages of the present analytical combination.

Keywords: THz spectroscopy, archaeological bronze, LIPS

1.Introduction

Archaeological bronzes typically present stratified earthy concretions and corrosion compounds. The latter often include reddish Cu(I) (cuprite) and/or blackish Cu(II) (tenorite) oxides with dispersed nantokite in close proximity of the metal substrate, along with Cu-carbonates, Cu-sulphates, and Cu-hydrochlorides at the outer layers, which produces the characteristic greenish appearance. The thicknesses of these mineral layers determine the overall degree of corrosion of archaeological copper alloys, which can be very variable, ranging from pseudomorphic oxidation with minimal alteration of the original surface to the destruction of the latter and the complete mineralisation of the metal walls [1].

The characterisation of the state of conservation of a given metal artefact has a crucial importance whenever approaching the analysis of its alloysusing non-destructive techniques such as X-ray fluorescence (XRF) and Particle Induced X-ray Emission (PIXE) or a micro destructive method such as laser induced plasma (or breakdown) spectroscopy (LIPS or LIBS). In general, for archaeological bronzes LIPS depth profiles can provide more reliable compositional information than XRF and PIXE since the former can analyse the metal bulk up to several hundred microns whereas the corresponding range of the latter is limited to several tens of microns. However, LIPS can only provide indirect information on the presence and condition of the metal substrate beneath the earthy concretions and corrosion stratifications, through the examination of the behaviour of the elemental profiles. Thus, the preliminary selection of the best areas to analyse by means of an effective method providing information on the material strata, as well as on the presence and position of the metal surface beneath the stratification, would be very helpful. Moreover, such a non-invasive

microstratigraphic characterisation of archaeological bronzes could also be very useful in order to design suitable conservation-restoration treatments.
Within this framework, here, we explore the potential of THz spectroscopy for collecting the mentioned stratigraphic information before LIPS analysis and any material removal conservation treatment. THz waves allow distinguishing different dielectric layers, which reflect the wave packet (echo signals) according to their corresponding refractive indexes. As each pulse corresponds to each layer, from which depth profiling can be obtained by using the time of flight method. To date, no alternative micro tomographic approaches are available for such a challenging characterisation, since optical methods are inapplicable while X-ray or neutron imaging do not offer enough discrimination and resolution, respectively.
Along the last decade, several applications of the THz-time domain spectroscopy (THz-TDS) have been pioneered in various fields by exploiting their potential to distinguish different dielectric layers. In particular,THz TDS has been used as non-destructive tool in biomedical engineering [2], physics [3], astronomy [4], communications [5], genetic engineering [6], pharmaceutical quality control [7], medical imaging [8], defence and security [9], and cultural heritage [10]. In the latter field THz spectroscopy and imaging have been successfully used for characterising paint layers [11][12][13], parchment and papyrus manuscripts [14][15], whereas only a preliminary work was reported on archaeological bronzes [16].
In this work, THz spectroscopy has been used for characterising a set of laboratory samples. These were suitably prepared in order to measure refractive indexes of some minerals of interest, roughly simulate the mineralisation stratigraphy, and investigate the corresponding reflection behaviours. Hence the THz reflectometry has been applied on a set of authentic archaeological bronze artefacts where complex behaviours were observed, depending on surface texture and corrosion phenomenology. LIPS elemental depth profiles were measured in the same spots of the THz TDS analyses in order to investigate possible correlations between the behaviours detected by these two complementary spectroscopic approaches. The discussion of the results achieved allows drawing some general conclusions on the archaeo-metallurgical potential of the THz spectroscopy and on exploitation of the present analytical combination.

2. MATERIALS AND METHODS

2.1 Terahertz time domain spectrometer

A commercial THz Time Domain Spectrometer (TDS) with a bandwidth of 0.1-2.5 THz was used in the present study. The system is equipped with a 1.550 µm ultrashort fiber laser with a pulse duration <80 fs (FemtoFErb 1560 produced by Toptica). A 50/50 splitter divides the laser beam into two channels terminated with LT-GaAs based photoconductive antennas (PCAs): emitter and detector, respectively. The single mode fiber-pigtailed design allows for a flexible arrangement in either transmission or reflection geometry. Both the PCAs are coupled to an elliptical silicon lens and then to a hemispherical TPX lens for collimating/focusing and focusing/collimating the THz beam [17][18].
The emission path includes a fast scanning delay stage. In order to vary the arrival time of the signal with respect to the pulse used for detection, a delay stage is introduced in the generation arm. By scanning the delay line, the phase and the electric field amplitude of the THz waveform can be sampled as a function of time. A LabView® software registers and saves the electric field amplitude from a digital lock-in amplifier that measures the signal from the detector.

Laser, fiber splitter, delay stage, driver electronics, power supply as well as the system control and data acquisition are all housed in one box (60 x 60 x 25 cm). The system is equipped with an USB data interface to allow versatile control via Labview® software.
The present measurements were carried out using the reflection geometry by fixing the incident and collection angles at about 30° to the sample surface normal, the corresponding plane, and focal position. To this goal the PCAs were mounted in a suitable yoke and an aiming laser beam was used in order to control the focus position. This set up allowed to rule out the typical alignment procedure using a metallic mirror and guaranteed a very good reproducibility.
The diameter of the THz beam at the focus position was measured using the knife-edge technique. Once the system has been optimized, a smooth metal edge is inserted in the beam at the test point and it is translated across the beam, gradually obscuring it. The THz signal is recorded at consecutive knife-edge positions. The maximum of the time domain peak may be plotted against the edge position, and for a perfect Gaussian beam the dependence is the well known error function. Once the data have been fitted, the beam waist (i.e. the spot diameter at the focus position) can be calculated.

2.3 Surface Roughness

In this work THz reflection TDS has been used to analyse the corrosion layers of a set of bronze archaeological objects. Generally significant amplitude decrease and broadening were observed on the reflection peaks of their outer layers. These phenomena appeared to be strongly dependent on the surface morphology thus a dedicated insight was carried out. Surface textures were measured using a 3D digital microscope [19][20][21] based on the shape from focus technique. A stack of images of the same scene, are acquired at different focal plane (i.e. heights). All the images are then processed in order to extract all the pixels in focus. These are correlated to the heights at which the images have been taken and a 2D data height map is readily obtained, which allows calculating the surface roughness parameters according to the well-known formulas.
In order to compute the roughness of the sample within the THz spots, evaluation areas of about 2x2 mm were framed with the 3D microscope around the THz spots, which were highlighted by the laser pointer.

2.4 Samples

Multilayer samples have been prepared in order to roughly simulate the actual corrosion stratigraphy in which the metal surface is covered by layers of copper corrosion products. We have firstly considered the case of two superimposed artificial layers placed on a suitable clamp to eliminate possible air gaps: a small slab of copper mineral (such as malachite, tenorite or cuprite) achieved using a press on a copper plate (0.5 mm thick). In a second set of samples we replaced the mentioned copper plate with an archaeological bronze fragment, which presented surface roughness higher than the copper plate. More complex situations have been also simulated including three layers: cuprite and malachite on a copper plate or the archaeological bronze.

2.5 LIPS

The THz microtomographic imaging has been combined with laser induced plasma spectroscopy (LIPS) elemental depth profiling. LIPS can perform depth profile analysis by

applying a series of subsequent laser pulses on the same spot area of the object thus providing chemometric information on the outer layers and the bulk of the object under study. This makes LIPS one of the most suitable technique for probing the distribution of elements in archaeological objects such as bronzes, where traditional sampling would produce unacceptable damages. However, LIPS is a micro-destructive technique (the diameter of the crater ranges between about 120-250 μm for a number of pulses of about 100 and 2000 respectively) and then it would be desirable to perform a limited number of measurements according to a suitable preliminary selection of the measurement site, in order to achieve a representative elemental characterizations of the artefact. In particular, archaeometrical studies of copper alloy artefacts [22], which presented deep corrosion and mineralization phenomena, have highlighted the limitations of "blind" choice of the LIPS measurement sites. Thus for example, the thickness of the corrosion layer in some parts of the object can be relatively large thus preventing LIPS from reaching the metal bulk. In this work we show as the knowledge in advance of the layer structure via THz imaging can allow a careful selection of LIPS measurement sites and provide a stratigraphic characterization, which can be usefully integrated with the elemental depth profiling.
LIPS measurements were performed using the set-up described in details elsewhere [23]. Shortly, it is equipped with a Q-Switching Nd:YAG (1064 nm) laser, four high resolution Czerny-Turner spectrometers (2.400 grooves/mm) combined with CCD linear array detectors, which cover the spectral range between 200-630 nm with a resolution of about 0.1 nm. The system has been calibrated for the analysis of copper alloy artefacts, also taking into account some depth-dependent phenomena affecting the response of the system in deep depth profile measurements [24].

3 RESULTS AND DISCUSSION

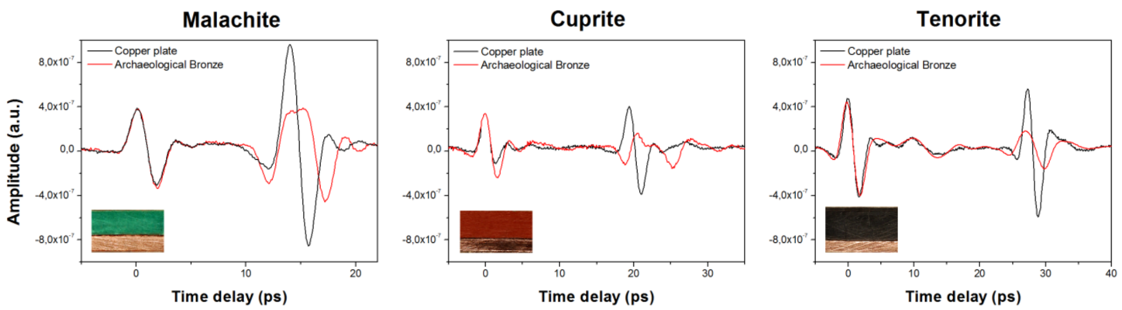

Fig. 1. THz signals reflected by two layers samples made with parallel slabs of corrosion products (malachite, cuprite and tenorite) placed on metal surfaces exhibiting different roughness (copper and archaeological bronze plates). The thickness of the parallel slabs is 0.8, 1.2 and 1.4 mm and the measured refractive index is 3.0, 2.7, 3.3 for malachite, cuprite and tenorite, respectively. The cross sections of corrosion products layers on copper plate are shown in the insets.

In Fig.1 the THz signals reflected from double layers samples (parallel slabs of copper minerals on smooth copper plate and archaeological bronze, respectively) are compared. All of them include two peaks of different amplitudes and shapes. Part of the incoming THz pulse is reflected at the first interface (i.e. air/corrosion material) and is responsible of the first peaks shown in Figs.1, whose different amplitudes is determined by the different refractive indexes of the minerals. The remaining part of the incoming THz pulse is transmitted through the mineral slab, reflected by the metal surface, transmitted back through the former, and eventually detected by the receiving PCA. The specular metal reflection was hence responsible of the second peaks of Figs. 1, whose amplitude was very sensitive to the alignment conditions. As shown, the reflection peaks of the copper surface had the same shape as those of the outer mineral surfaces and higher amplitudes with respect to the latter. Conversely, the shapes of the reflections by the archaeological bronze surface appeared variable and with a significantly lower amplitude with respect to those by the copper plate.

These different behaviours can be interpreted by considering that the THz pulse experiences different reflections when it encounters a smooth or a rough surface beneath the mineral layer.

Here, the average roughness (according to the DIN standard), as measured using the 3D microscopy introduced above, was 5 and 38 microns for the copper and the archaeological bronze plates, respectively.The former is that of the metal surface while the latter is that of the mineralised bronze surface, which provides a qualitative information on the corresponding roughness of the metal underneath. Thus, in the smooth case, the specular component prevails, and no leakage of signal is observed by the detector. In the rough case, the reflection from the metal surface is not specularand the signal is mainly attenuated and distorted by complex scattering phenomena due to the metal asperities and random of the corrosion products. Therefore, the reflected signal is diffused within a wider angle than the specular case, and most part does not hit to the detector, which was placed in the specular position. This means that the ability of THz to locate the presence of the metal beneath the corrosion layers is strongly dependent on its state of conservation (i.e. its roughness and waviness of the order of the beam size).

The previous analysis has been extended to a more complex sample: a three layer made of parallel slabs of cuprite, malachite on a metal substrate (copper and archaeological bronze laminas). In Fig. 2, three peaks are visible. The first two are due to the air/cuprite and cuprite/malachite interfaces respectively. The third peak is originated at the malachite/metal interface. As for the two layers-samples, the amplitude of the third peak is determined by the specular component of the reflected beam, and multiple reflections are negligible.

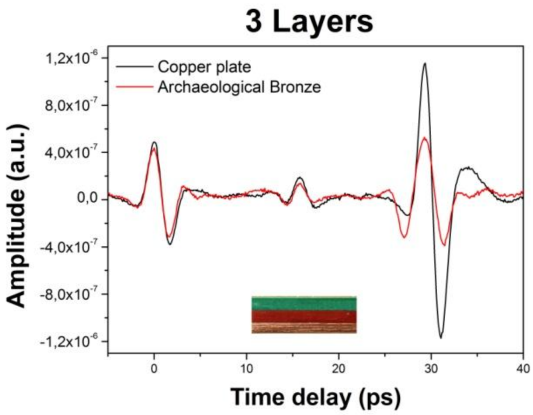

Fig. 2. THz reflection signals from a three layer sample made with cuprite, malachite (both 0.8 mm thick) and metal surfaces (copper and archaeological bronze plates). The cross section of corrosion products layers on copper plate is shown in the inset.

As for the double layer samples, the reflection pattern was more complex with original archaeological lamina because of its complex surface texture and deterioration phenomenology [1]. The above described preliminary measurements on the mock-ups were very useful in order to interpret the THz characterization of authentic archaeological findings described below.

The first original sample investigated using THz TDS and LIPS was a small fragment (21x29 mm maximum sizes, Fig. 3 a)) from the archaeological site of Vada (Livorno, Italy). This fragment appeared as a mineral stratification mostly including chlorides and malachite covered with a thin earthy encrustation, without any visible evidence of the metal substrate. The THz characterisation was hence mainly aimed at assessing the presence of the latter.

The plots in Fig. 3b)) report the THz reflection patterns registered in the two indicated spots, which show a single broadened and structured peak, which is attributable to the superposition of the reflections at outer material layers of the sample, but no metal reflection was pointed out. An internal reflection due to differences of refraction indexes was detected at the site 2 but its amplitude was too low to be attributed to the metal substrate. This demonstrated the full mineralisation of the fragment, which was also supported by the very low weight of the present finding, although the possible presence of minute metal relicts cannot be ruled out.

Despite any trace of metal substrate was detected by THz in the site 1 (Fig. 3 a)), the corresponding LIPS depth profile (Fig. 3 c)) of tin exhibited the typical behavior of archaeological bronzes: surface enrichment followed by a stabilization towards the bulk content, which is accompanied by a simultaneous decrease of hexogen elements such as calcium. However, the inner tin content provided by LIPS in the present case (about 7.5 wt%) does not correspond to that of the original copper alloy but rather to its mineral residues. The only hint suggesting the possible absence of metal substrate is provided by the fluctuations of the tin content, which were significantly higher than the typical ones of preserved archaeological copper alloys.

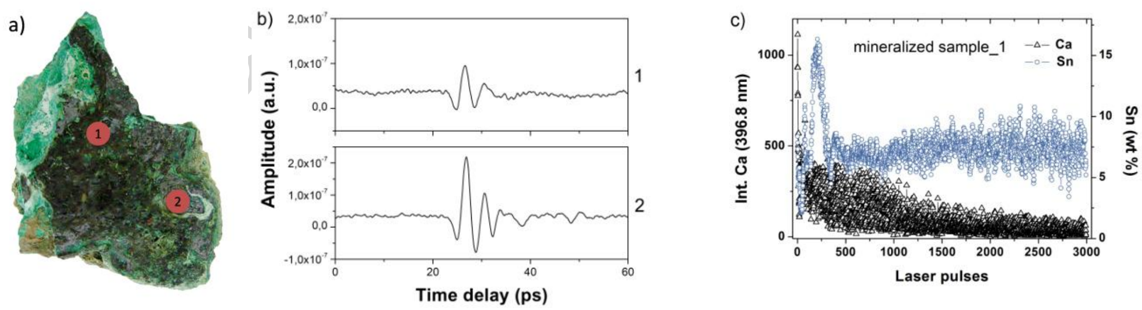

Fig. 3. a) fully mineralized sample; b) THz signals reflected from points 1, 2; c) LIPS depth profiles in correspondence of the THz measurement 1.

The second archaeological object investigated in the present study was a 62 mm diameter decorative bronze stud from Cuba, which was partially cleaned. The roughness of its metal surface appeared as cast with a high roughness (more than 100 microns average roughness).

In Fig. 4 a) three areas of the object are evidenced: 1) after deep cleaning, 2) after light mechanical cleaning, and 3) as it was (the area is greenish due to the significant presence of chlorides). The plots b) in Fig. 4 show the THz reflections from points on areas 1, 2 and 3. The peaks reflected from area 2 appear to be more attenuated and broadened as compared to

the peak from the area 1. The lowermost plot in Fig. 4 b) represents the THz signal reflected by a point on the rough unclean surface (area 3). Two peaks can be observed. The first peak appears to be broadened and it is due to the interface air/chlorides while the second one arose from the reflection at the chlorides/metal interface. As this is a thin chlorides layer, the first and second peaks are not well separated, in other words the second peak partially overlaps the first peak, and only the negative lobe of the second peak can be evidenced. The second peak results to be more attenuated than the first peak. In this case theTHz signal decreases because some reflections are not detected by PCA in specular geometry, in other words these reflections do not fall within the acceptance angle of the detector.
Tin LIPS depth profiles of both sites 1 and 3 (Fig. 4 c)) exhibited a slight surface enrichment an a rapid decrease of concentration towards the bulk value (about 3.1 wt%). The amplitude of the tin content fluctuations was one order of magnitude lower than the previous case.

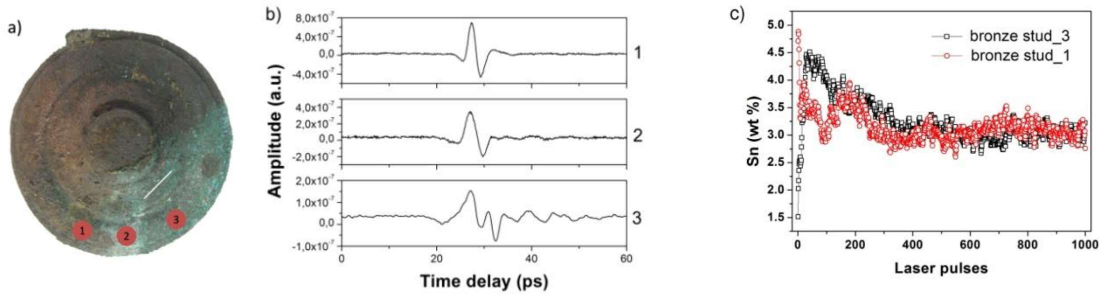

Fig. 4. a) bronze stud; b) THz signals reflected from points 1, 2 and 3; c) LIPS depth profiles in correspondence of THz measurements 3 and 1.

The third sample was an engraved bronze lamina (46x19 mm) from the mentioned excavation of Vada. It is made of bronze covered by a dark patina and residual of earthy encrustation. One side of this object presented earthy encrustation (area 1) while the other one was cleaned using laser ablation, as shown in Fig. 5 a) (area 2). The reflection THz patterns from the former area was a broad and structured peak of moderate intensity, whereas a narrow and intense peak was detected from the latter (Fig. 5 b)). The broadening has to be reasonably attributed to the path differences associated with the higher roughness of the area 1.

The presence of the metal beneath the encrustation and corrosion layers is evidenced by the presence of two superimposed peaks (uppermost plot in Fig. 5 b)).

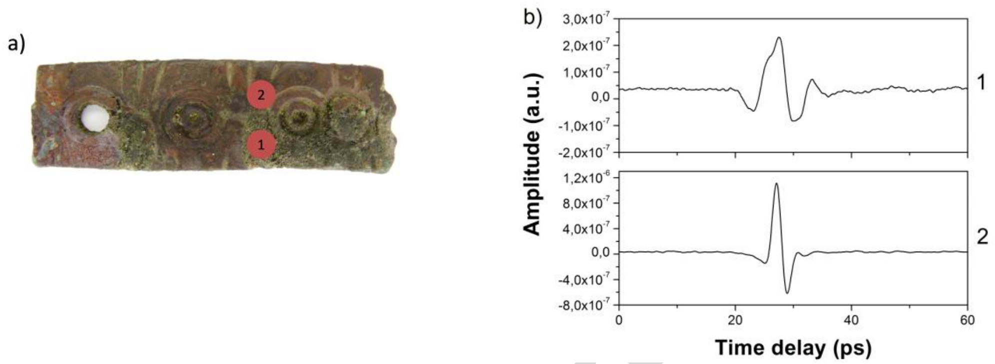

Fig. 5. a) decorated rectangular plate; b) THz signals reflected from 1 and 2.

The fourth finding was a bronze plaque from the Vada excavation (90x42 mm). Similarly to the previous object, the surface was partially covered by hard earthy concretions (area 3 in Fig. 6 a)) and partially cleaned using laser ablation (area 1) and scalpel (area 2). The latter treatment reduced the thickness of the concretion while the former uncovered the reddish cuprite layer which represents the level of the original surface.

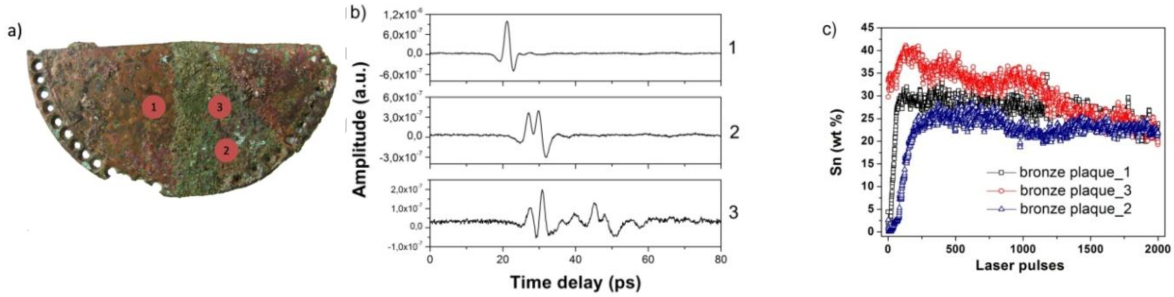

Fig. 6 a) bronze plaque; b) THz signals reflected from 1, 2, 3; c) LIPS depth profiles in correspondence of the THz analyzed area.

The plot 1in Fig. 6 b) shows the THz signal reflected by a point in the cleaned surface (area 1): the amplitude of this peak was about one order of magnitude higher than the peak reflected from points in the areas 2 or 3, which highlights the occurrence of a specular reflection in the zone 1. It is interesting to note the double peak of the plot 2 in Fig. 6 b). The time difference between the first and the second peak can be related to the thickness [18] of the concretion (corrosion products and earthy material) left on the metal surface after scalpel removal. Assuming reasonable a refractive index of the corrosion layer of 3, the estimated thickness is less than 200 microns. Similarly, in the plot 3 of Fig. 6 b) the presence of the metal interface was about 20 ps after the air/corrosion layers interface. In this case the estimated thickness was about 1000-2000 microns as measured with 3D microscopy. The comparison of the tin depth profiles (Fig. 6 c)) of the three areas of Fig. 6 a) shows the congruence of the bulk content measured while some differences were observed among the compositional variations, which were larger in the encrusted zone (area 3).

Finally a bronze figurine (Fig. 7) from Florence's Egyptian Museum (Osiris inv. 5458) has been investigated. On the basis of the previous THz characterisation of samples with known or relatively simple stratigraphy, we tried in this case to assess whether there were zones with preserved metal bulk beneath the corrosion strata, which could be analysed using LIPS.

The THz pulse echo image in the Fig.7 was achieved by measuring the reflected pulses along the white line depicted on the bronze figurine.

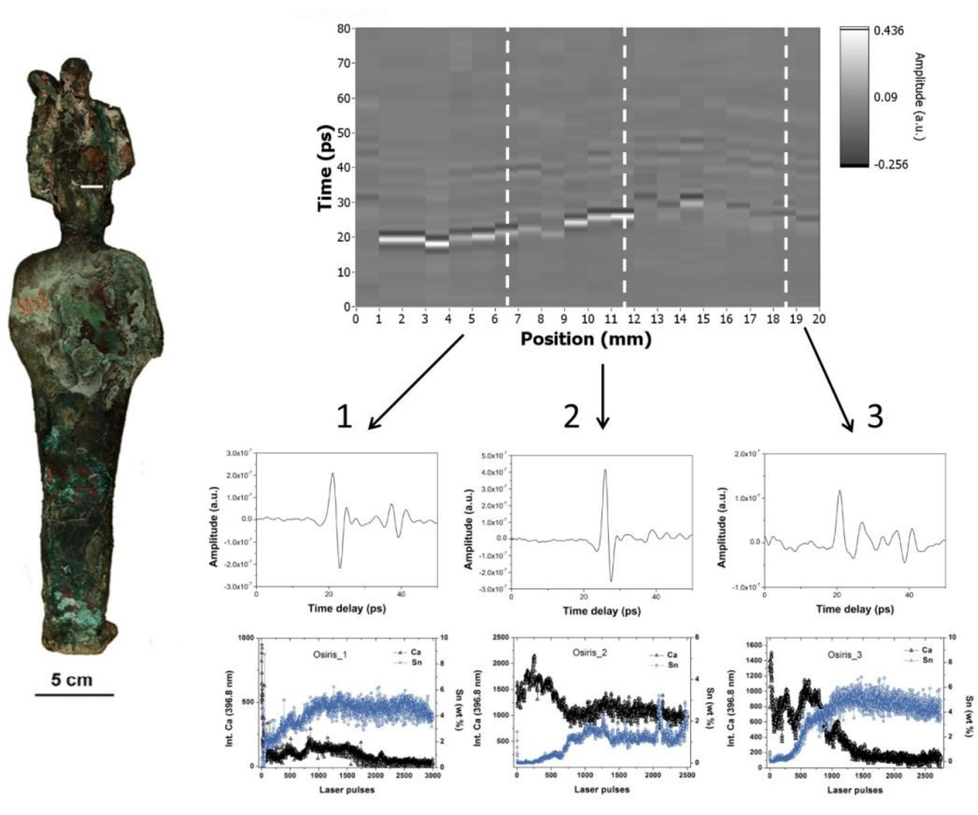

Fig. 7. Upper left) bronze Egyptian figurine (Osiris inv. 5458); upper right) echo pulse image and THz signals reflected from bronze beneath corrosion layers, and from a mineralization area with high stratification; bottom) LIPS elemental depth profiles on three sites in correspondence of THz measurements with different degree of corrosion.

The plots in Fig. 7 show the reflection patterns detected included the main reflection by the air/corrosion layers interface and a sequence of peaks, which evidenced the high stratification of the corroded wall probed. Nevertheless, according to the discussion of the behaviours of the previous samples, the presence of the peak around 40 ps allowed arguing for the sites 1 and 3 the correspondent presence of the metal bulk, whereas this was not observable in the site 2. Such a preliminary characterisation was congruent with the LIPS analyses in the same sites. The profiles 1 and 3 presented a rising tin content, which is typically observed in very corroded archaeological bronzes with a deep outer layer of cuprous oxides, and a decreasing exogenous calcium content, which disappeared after about 2000 laser pulses. In both cases the tin content approached to about 4 wt% and remained relatively stable for a large number of laser pulses. The preliminary THz probing allowed us to consider this value as the tin content of the bulk. Conversely, an anomalous behaviour was observed in the site 2, where the tin content presented strange peaks up to 3000 laser pulses and assumed the maximum value of about 2 wt%. Furthermore, the persistence of a high content of Ca, strengths the evidence of the absence of the metal bulk already highlighted by THz reflection TDS.

The outer layer thickness was measured with both THz reflectometry and LIPS, and a very good agreement was found. As an example, the time difference between the THz reflected pulses from site 1 was about 20 ps, considering a refractive index of 2.7, the layer thickness was found to be 1283 μm. On the same site we applied two sets of pulses with different ablation rate. As a rough estimation, the first 100 pulses were applied at 3 μm/pulse and the second 1000 pulses at 1 μm/pulse. The layer thickness estimated with LIPS measurements was found to be 1300 μm.

4 Conclusions

In this work we showed the microstratigraphic characterization of corroded bronzes using THz TDS reflectometry is a difficult task. The waviness of the material interfaces encountered by the beam can play a crucial role whenever it produce changes of the incidence angle and then attenuation and broadening of the detected reflected pulse. This hold for both the corrosion layers and the metal substrate where the latter is still preserved. The metal asperities can produce peaks of very variable amplitude according to the random surface texture produced by corrosion processes. These geometric effects along with the complex superposition and intertwine of the copper alloy corrosion layers make the technique not suitable for achieving precise microtomographic reconstructions. On the other hand, the present investigation shows the THz reflectometry can be very useful in order to preliminarily assess the presence of the metal bulk beneath encrustations and corrosion layers before performing compositional analyses using LIPS, as well as other non-destructive (ex. XRF, PIXE) or microdestructive (ex. microsampling) technique. The standalone application of any of these techniques for measuring the alloy compositions can provide misleading data if not associated with reliable stratigraphic information.

Oncoming works will be dedicated to the study of the dependence of the reflection patterns as a function of the THz beam diameter in order to define and optimize a measurement protocol for deeply corroded copper alloy artefacts.

5 Acknowledgements

The authors gratefully acknowledge the financial support by Regione Toscana, “Fondo per le infrastrutture produttive”, D.G.R.T. n. 924 - 19/10/2009.

6. References

[1] D. A. Scott, Copper and bronzes in art, Getty Publications, Los Angeles 2002.

[2] K. Humphreys, J. P. Loughran, M. Gradziel, W. Lanigan, T. Ward, J. A. Murphy, C. O'sullivan, "Medical applications of terahertz imaging: a review of current technology and potential applications in biomedical engineering", Conf. Proc IEEE Eng. Med. Biol. Soc. pp. 1302-5, 2004.

[3] R. A. Lewis, "A review of terahertz sources", J. Phys. D, v. 47, pp. 374001(11), 2014.

[4] G. J. Stacey, "THz Low Resolution Spectroscopy for Astronomy", IEEE Trans. THz Sci. Technol., v. 1, pp. 241-255, 2011.

[5] G. C. Righini, I. Cacciari, A Tajani, and M. Brenci, "Terahertz flexible waveguides: an overview", Proc. SPIE 7366, pp. 73660Z1(11), 2009.

[6] J. E. Grundt, C. Cerna, C. C. Roth, B. L. Ibey, "Terahertz radiation triggers a signature gene expression profile in human cells", Infrared, Millimeter and Terahertz Waves, 36th International Conference on, pp. 1-2, 2011.

[7] S. Fan, Y. He, B. S. Ung and E. Pickwell-MacPherson, "The growth of biomedical terahertz research", J. Phys. D Appl. Phys., v. 47, pp. 374009(11), 2014.

[8] C. Yu, S. Fan, Y. Sun, E. Pickwell-Macpherson, "The potential of terahertz imaging for cancer diagnosis: A review of investigations to date", Quant. Imaging Med. Surg., v. 2, pp. 33-45, 2012.

[9] H.-B. Liu, Z. Hua, N. Karpowicz, Y. Chen, Z. Xi-Cheng, ", Terahertz spectroscopy and imaging for defense and security applications", Proceedings of the IEEE, v. 95, pp. 1514–1527, 2007.

[10] J. B. Jackson, J. Bowen, G. Walker, J. Labaune, "A Survey of Terahertz Applications in Cultural Heritage Conservation Science", IEEE Trans. THz Sci. Technol, v. 1, pp. 220-231, 2011.

[11] J. B. Jackson, M. Mourou, J. F. Whitaker, I. N. Duling III, S. L. Williamson, M. Menu, G. A. Mourou, "Terahertz imaging for non-destructive evaluation of mural paintings", Opt. Commun. v. 281, pp. 527-532, 2008.

[12] D. Giovannacci, D. Martos-Levif, G. C. Walker, M. Menu, and V. Detalle, "Terahertz applications in cultural heritage: case studies", Proc. SPIE 9065, pp. 906510(7), 2013.

[13] R. Radpour, N. Bajwa, J. Garritano, S. Sung, M. Balonis-Sant, P. Tewari, W. Grundfest, I. Kakoulli, Z. Taylor," THz imaging studies of painted samples to guide cultural heritage investigations at the Enkleistra of St. Neophytos in Paphos, Cyprus", Proc. SPIE 9199, pp. 91990Q1(9), 2014.

[14] K. Fukunaga, Y. Ogawa, S. Hayashi, I. Hosako, "Terahertz imaging for analysis of historic paintings and manuscripts", Infrared, Millimeter and Terahertz Waves, 33th International Conference on, pp. 1-13, 2008.

[15] J. Labaune, J. B. Jackson, S. Pagès-Camagna, I. N. Duling, M. Menu, G. A. Mouro, "Papyrus imaging with terahertz time domain spectroscopy", Appl. Phys. A, v. 100, pp. 607-612, 2010.

[16] J. B. Jackson, J. Labaune, G. A. Mourou, L. D'Alessandro, A. Whyte, M. Menu, "Pulsed terahertz investigation of corroded and mineralized copper alloy historical artifacts", Infrared, Millimeter and Terahertz Waves, 36th International Conference on, pp. 1-2, 2011.

[17] I. Cacciari, S. Siano, "THz spectrometer with fiber coupled antennas: Preliminary application test for characterizing stone artefact", Photonics Technologies, pp. 1-4, 2014.

[18] I. Cacciari, D. Ciofini, S. Siano, "THz characterization of painting layers", Fotonica AEIT Italian Conference on Photonics Technologies, pp. 1-4, 2015, DOI: 10.1049/cp.2015.0170.
[19] I. Cacciari, D. Ciofini, M. Mascalchi, A. Mencaglia, S. Siano, "Novel approach to the microscopic inspection during laser cleaning treatments of artworks", Anal. And Bioanal. Chem. v. 402, pp. 1585-1591, 2011.
[20] I. Cacciari, P. Nieri, S. Siano, "3D Digital Microscopy for Characterizing Punchworks on Medieval Panel Paintings", Journal on Computing and Cultural Heritage, v. 7, pp. 1-15, 2014.
[21] I. Cacciari, A. A. Mencaglia, S. Siano, "Micromorphology of gold jewels: a novel algorithm for 3D reconstruction and its quality assessment", Proc. SPIE 8790, pp. 87900B1(9), 2013.
[22] J. Agresti, I. Osticioli, M. C. Giudotti, G. Capriotti, N. Kardjilov, A. Scherillo, S. Siano, "Combined neutron and laser techniques for technological and compositional investigations of hollow bronze figurines", J. Anal. At. Spectrom., v. 30, pp. 713-720, 2015.
[23] J. Agresti, A. A. Mencaglia and S. Siano, "Development and application of a portable LIPS system for characterising copper alloy artefacts", Anal. Bioanal. Chem, v. 395, pp 2255-2262, 2009.
[24] J. Agresti, S. Siano. "Depth-dependent calibration for quantitative elemental depth profiling of copper alloys using laser-induced plasma spectroscopy", Appl. Phys. A, v. 117, pp. 217-221, 2014.

Highlights

1) We use THz to assess the presence of metal bulk on archaeological bronze
2) We use THz to characterize material strata
3) We show how THz results are used before performing compositional analyses (LIPS)
4) The state of conservation of metal beneath corrosion layers determines THz efficiency